INITIAL RATE OF SECONDARY COMPRESSION IN ONE-DIMENSIONAL CONSOLIDATION ANALYSIS

Toshihiko Takeda [1], Motohiro Sugiyama [2], Masaru Akaishi [2], and Huei-Wen Chang [3]

ABSTRACT

The finite difference analysis of one-dimensional consolidation of clays, exhibiting large amounts of secondary compression during primary consolidation, provide fairly good predictions of the consolidation-time curve for oedometer specimens with different heights. Some parameters including the initial rate of secondary compression defined by primary consolidation in this analysis have been assumed to avoid experimental difficulty. The trial and error calculation procedure was therefore used where the calculated consolidation-time curves fit the observed ones. Finally, it is emphasized that the assumption for unknown secondary compression behaviors during primary consolidation has a predominant influence on the consolidation-time curve.

Key words: One-dimensional consolidation, rate of secondary compression, H^2 scaling law.

1. INTRODUCTION

The theory of one-dimensional consolidation proposed by Terzaghi (1943) has been widely used to predict the settlement-time relation of soft grounds. From both field and laboratory observations, it is well known that the actual consolidation behavior differs from the prediction based on the Terzaghi's theory. It has been suggested that one of the reason for this difference between the consolidation test results with the theoretical prediction may be due to the effect of the so-called secondary compression which is not considered in the Terzaghi's theory.

Figure 1 shows the typical settlement-time curves (Aboshi 1973). One-dimensional consolidation settlement has been traditionally divided into primary and secondary compression component. As shown in Fig. 1, the settlement under sustained load continues almost indefinitely but the primary component would reach its ultimate settlement at the end of primary consolidation (t_{EOP}). Secondary compression may occur during the primary consolidation period though it is more noticeable after primary consolidation is completed (Taylor 1948). Secondary compression observed after the end of primary consolidation, form an approximately linear relationship when plotted against the logarithm of time (Mesri and Rokhsar 1974; Murakami 1977; Feng 2010). The studies on secondary compression based on the time dependent soil model are extensive. Although some of secondary compression soil models are expressed by a function of time and effective stress, Leroueil *et al*. (1985) pointed out that a major difficulty encountered with these models is that the origin of time must be defined. However, this difficulty can be overcome by a unique stress-strain-strain rate model. To avoid the difficulty of determining the time origin for secondary compression, Yin and Graham (1996) introduced a concept of a reference time line indicating the duration of secondary compression. However, these discussions are doubtful because only the total compression which consists of both the primary and secondary compression, can be read on dial gauges in conventional consolidation test. It is impossible to measure separately the secondary compression from the total compression during primary consolidation. Consequently, the secondary compression behaviors during primary consolidation cannot be fully understood with the experimental evidence.

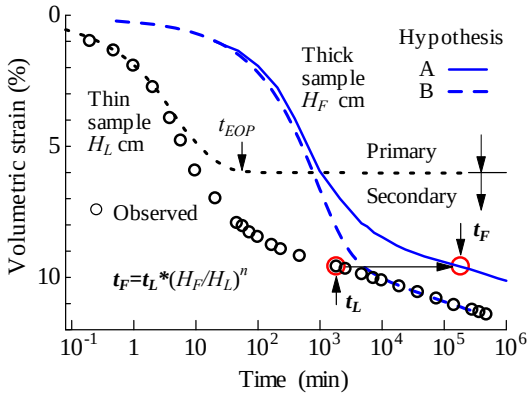

Fig. 1 Hypotheses A and B for settlement-time curves of one-dimensional consolidation (Aboshi 1973)

Ladd *et al*. (1977) presented two extreme cases, namely hypotheses A and B for the time effects in one-dimensional consolidation as shown in Fig. 1. Hypothesis A assumes the secondary compression occurs only after the end of primary consolidation (t_{EOP}) and the settlement-time curve of the thick sample is simply displaced in proportional to the squared ratio of the drainage distance $(H_F / H_L)^2$. Hypothesis B is based on Suklje's isotaches theory (1969) which assumes that the settlement-time curves of both thin and thick samples coincide with each other in secondary compression stage. However, the experimental data presented by Mesri *et al*. (1995) and Aboshi (1973) supports hypothesis A rather than B and the existence of secondary compression during

Manuscript received April 17, 2013; revised June 24, 2013; accepted June 28, 2013.

[1] General Manager, Onoda Chemico Co., Ltd. Yokohama City 231-0027, Japan (e-mail: t_takeda@chemico.co.jp).

[2] Professor, Department of Civil Engineering, Tokai University, Hiratsuka City, 259-1292, Japan (e-mail: sugi@keyaki.cc.u-tokai.ac.jp; redstones_3710812@yahoo.co.jp).

[3] Professor (corresponding author), Department of Civil Engineering, National Central University, Jhongli City, Taiwan (e-mail: hueiwen@cc.ncu.edu.tw).

primary consolidation. On the contrary, Nash (2001), Imai *et al*. (2003), and Haan and Kamao (2003) reported the validity of the isotaches theory in one-dimensional consolidation. It may be said that while many theories have been published for secondary compression, none has been generally being accepted for discussion (consistently) on the rate of the secondary compression during the primary consolidation, since there is no experimental evidence available.

Takeda *et al*. (2012) had proposed a constitutive equation in the form of $F(e, p, \partial e / \partial t) = 0$ for the one-dimensional consolidation analysis. In this paper, the void ratio rate $\partial e / \partial t\ (= \dot{e})$ of our proposed model rewrite in the time rate of the total volumetric strain $\partial v / \partial t\ (= \dot{v})$ in order to make it more convenient. It is the purpose of this paper to examine not only the influence of secondary compression developed during primary consolidation on the consolidation-time curve, but also to consider how to assume the initial rate of secondary compression in the numerical consolidation analysis. It is shown that the curve fitting procedures described in this paper provide a method of one-dimensional consolidation analysis taking account of secondary compression.

2. CONSOLIDATION EQUATION AND SECONDARY COMPRESSION MODEL

The equation that governs the process of consolidation is expressed as follows (Terzaghi 1943):

$$\frac{\partial v}{\partial t}(= \dot{v}_p + \dot{v}_s) = -\frac{k}{\gamma_w}\frac{\partial^2 u}{\partial t^2} \tag{1}$$

where $\partial v / \partial t\ (= \dot{v})$ is the time rate of the total volumetric strain as the sum of primary and secondary volumetric strain rate, $\dot{v}_p$ and $\dot{v}_s$ respectively, k is the permeability, γ_w is the unit weight of water, u is the excess pore water pressure, y is the vertical coordinate and t is the time.

The effective stress-total volumetric strain-strain rate relationship is given for the component of primary and secondary compression as follows (Sekiguchi and Torihara 1976; Shirako *et al*. 2008):

$$\Delta v(= \Delta v_p + \Delta v_s) = \frac{\lambda}{f_0}\ln\left(\frac{p}{p_0}\right) = \frac{\lambda^*}{f_0}\ln\left(\frac{p}{p_0}\right) + \alpha\ln\left(\frac{\dot{v}_0}{\dot{v}_s}\right) \tag{2}$$

where λ and λ^* are the compression index defined by the total and primary compression respectively, f_0 is the initial specific volume, p is the vertical effective stress, p_0 is the vertical effective overburden stress, α is the coefficient of secondary compression defined by the volumetric strain and $\dot{v}_0$ is the initial rate of secondary compression.

The rate of the volumetric strain due to the primary consolidation and secondary compression can be derived from Eq. (2).

$$\dot{v}_p = \frac{\lambda^*}{f_0 \cdot p}\dot{p} = -\frac{1}{K}\cdot\dot{u} \tag{3}$$

$$\dot{v}_s = \dot{v}_0 \cdot \exp\left(-\frac{(\lambda - \lambda^*)}{f_0}\ln\left(\frac{p}{p_0}\right)/\alpha\right) \tag{4}$$

where $\dot{p} = -\dot{u}\ (= -\partial u / \partial t)$ and $K = f_0 \cdot p / \lambda^*$.

Primary volumetric strain Δv_p occurs simultaneously with an increase in effective stress and the secondary volumetric strain Δv_s represents the reduction in volume under constant effective stress. Substitution of Eqs. (3) and (4) into Eq.(1), the continuity equation for the process of one-dimensional consolidation is rewritten as

$$\frac{\partial u}{\partial t} = c_v^*\frac{\partial^2 u}{\partial y^2} + K\cdot\dot{v}_s \tag{5}$$

where c_v^* is the coefficient of consolidation defined by the primary consolidation and is calculated by $c_v^* = k \cdot K / \gamma_w$.

A complete solution through the use of the finite difference method has been obtained for one-dimensional consolidation considering secondary compression. The finite difference approximations by differentiating Eq. (5) are

$$\frac{\partial u}{\partial t} \approx \frac{u_{i,t+\Delta t} - u_{i,t}}{\Delta t} \tag{6}$$

$$\frac{\partial^2 u}{\partial y^2} \approx \frac{u_{i+1,t} - 2\cdot u_{i,t} + u_{i-1,t}}{\Delta y^2} \tag{7}$$

where $u_{i,t}$ and $u_{i,t+\Delta t}$ are the excess pore pressure at point i and times t and $t + \Delta t$. Consequently, if written in the finite difference form, Eq. (5) becomes

$$u_{i,t+\Delta t} = u_{i,t} + M\cdot(u_{i+1,t} - 2\cdot u_{i,t} + u_{i-1,t}) + K\cdot\dot{v}_s\cdot\Delta t \tag{8}$$

where $M = c_v^*\cdot\Delta t / \Delta y^2 \le 0.5$ and the numerical solution converges if the time increment Δt and the spatial grid increment Δy are chosen such that M is equal to or less than 0.5 (Harr 1966).

The simple explicit solution is as follows:

(a) The excess pore pressures immediately after the application of an increment of load are calculated along a series of points and nodes throughout the consolidation layer.

(b) Using the excess pore pressure above and below the nodal point i at time t, $u_{i,t+\Delta t}$ is calculated from Eq. (8).

(c) Effective stress increment Δp_i at a nodal point i can be obtained from $\Delta p_i = u_{i,t+\Delta t} - u_{i,t}$.

(d) The rate of secondary compression $\dot{v}_s$ at a nodal point i can be calculated by Eq. (4).

(e) $K\cdot\dot{v}_s\cdot\Delta t$ in Eq. (8) is equivalent to the excess pore pressure increment developed by secondary compression and distributed to a nodal point i.

(f) The initial and boundary conditions for the analysis in this paper are identical with those in the oedometer test.

3. OUTLINE OF EXPERIMENTS AND SOIL PARAMETERS

3.1 Outline of Experiments

Long term oedometer tests were conducted on undisturbed Hitachi clay to examine secondary compression behavior. The geotechnical properties of Hitachi clay and the long term settlement of road embankment on the soft ground have been extensively investigated by Japan Highway Public Corporation (Tatta *et al*. 2003). Average physical properties for the clay are as follow; soil particle density ρ = 2.68 g/cm^3, natural water content $w_n = 100\%$, liquid limit $w_L = 114\%$, plastic limit $w_p = 48\%$. The undisturbed samples were carefully prepared by trimming it to fit into the oedometer ring, which were 6 cm in diameter and 2 cm in height. In order to investigate the influence of drainage distance, 1 cm and 0.7 cm in height samples were also prepared. The rings were lubricated with silicon grease to reduce friction and filter papers were placed on the top and bottom of the sample. The samples were normally consolidated under the pressures varied from the pre-consolidation pressure 78.48 kPa to 156.96 kPa and the amount of compression was measured.

This paper is only concerned with the verification of the basic assumption for secondary compression made by Eq. (4) and the evaluation of soil parameters involved from laboratory results.

3.2 Soil Parameters

Most of soil parameters required for one-dimensional consolidation analysis in consideration of secondary compression are calculated from the consolidation-time curve in the one-dimensional consolidation tests as shown in Fig. 2. But some of them cannot be determined by the experimental results (Takeda *et al*. 2012). The validity and the applicability of the assumed soil parameters are verified by the comparison of the calculated consolidation-time curves with the observed results. The procedure of determining soil parameters is as follows:

1. The compression index λ is calculated from the volumetric strain v_f of one day after.
   Sample No. 1:

$$\lambda = v_f \cdot f_0 / \ln(p / p_0)$$
$$= 0.0945 \times 3.191 / \ln(156.96 / 78.48) = 0.44$$

2. The coefficient of consolidation c_v is found by $\sqrt{t}$ method and it is assumed that $c_v^* = c_v$. The coefficient of consolidation c_v^* which should be determined from the primary compression-time curve cannot be determined from total compression-time curve as shown in Fig. 1.

$$c_v = T_v \cdot H^2 / t_{90} = 0.848 \times 0.888^2 / 13.7 = 0.049 \ (\mathrm{cm}^2/\mathrm{min})$$

3. The coefficient of secondary compression α is easily determined from the final slope of the semi-logarithmic plot of the consolidation-time curve after the primary consolidation has ended.

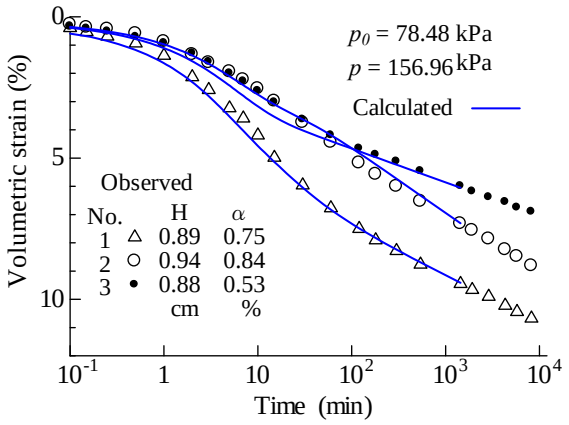

Fig. 2 Consolidation-time curves of observed and calculated results

$$\alpha = 0.434 \cdot \Delta v / \log(t_2 / t_1)$$
$$= 0.434 \times 0.0155 / \log(1440 / 180) = 0.00745$$

4. The value of compression index λ^* defined by the primary compression is arbitrarily assumed to be less than that of λ if the observed volumetric strain includes the secondary compression.
5. The initial rate of secondary compression, $\dot{v}_0$ is also assumed as follows;

$$\dot{v}_0 = \alpha / t_{90} = 0.00745 / 13.7$$
$$= 5.44 \times 10^{-4} (1/\mathrm{min}) \quad (9)$$

   where t_{90} is the time of 90% consolidation.

   The behaviors of secondary compression during the primary consolidation cannot be clarified by experiment, and this assumption infers that the notable secondary compression occurs after t_{90}. Besides, it should be noted that t_{90} is affected by the drainage distance. This contention will be discussed later in more detail. Thus, there are three unknowns, c_v^*, λ^* and $\dot{v}_0$ which cannot be determined by experiment.
6. Therefore, applicable values of these soil parameters are modified by a trial and error procedure until the calculated volumetric strain coincides with the observed one.

3.3 Consideration of Calculation Results

(1) Consolidation-time curves

Table 1 shows the soil parameters determined or assumed by the above-mentioned fitting procedure and the calculated consolidation-time curves are solid lines in Fig. 2. It is natural that the calculated volumetric strain v_f after one day is in agreement with an actual measurement. However, the consolidation process, namely, the consolidation-time curve for one day is fairly in agreement with the experimental result.

It can be seen from Fig. 2 that there are small deviations between the calculated and observed consolidation-time curves in the primary consolidation stage. To produce more consistent

Table 1 Soil parameters

No.	λ	λ*	c_v (cm²/min)	α (%)	$\dot{v}_0$ (1/min)	t_{90} (min)	λ*/λ	H (cm)
1	0.44	0.23	0.049	0.75	5.4×10^{-4}	13.7	0.53	0.888
2	0.39	0.13	0.045	0.84	4.9×10^{-4}	17.0	0.33	0.943
3	0.25	0.13	0.054	0.53	3.8×10^{-4}	12.0	0.52	0.884

result, it may be required to change the values of the soil parameters tabulated in Table 1. By using the revised coefficient of consolidation (Sample No. 3) which is reduced $c_v^* = 0.054$ cm²/min (denoted by a solid line) to 0.03 cm²/min (dash lines), one of consolidation-time curves shown in Fig. 2 was examined and plotted again as in Fig. 3. The shape of the dash line based on a suitable choice of c_v^* value agrees well with the experimental result. The volumetric strain-time curves in a pervious and impervious boundary are also shown in Fig. 3. Primary consolidation in a pervious boundary $y/H = 0$ has ended immediately after loading. The amount of primary compression is calculated correctly and confirmed from the early stage of consolidation. Therefore, a dash line for the pervious boundary is equivalent to the secondary compression-time curve. It can be found that the volumetric strain calculated by the model of Eq. (2) is proportional to the logarithm of time after roughly 100 minutes. Moreover, the volumetric strain-time curve in the impervious boundary, $y/H = 1$ coincide with that of the pervious boundary for the secondary compression stage.

(2) Influence of the initial rate of secondary compression $\dot{v}_0$

The rate of secondary compression with time in pervious and impervious boundary of the consolidation layer is shown in Fig. 4. In these calculations, the time increment of $\Delta_t = 3.3\times10^{-2}$ minutes is used and fixed in the whole consolidation process in the calculation. Primary consolidation in the impervious boundary $y/H = 1$ begins when the average degree of consolidation reaches to about 33%. Although the secondary compression has started before the consolidation has reached the 33% of the consolidation. The rate of secondary compression increases rapidly up to the initial value $\dot{v}_0$ immediately after the beginning of primary consolidation. The feature of a secondary compression model expressed with Eq. (2) can be observed from the calculated result shown in Fig. 4.

According to the model of Eq. (2), the rate of secondary compression decreases with the increase in secondary compression. The secondary compression occurred during the primary consolidation is dependent on an assumption of the initial rate of secondary compression $\dot{v}_0$. If the time of 90% consolidation t_{90} in Eq. (9) is replaced by t_{50} or t_{30}, the initial rate of secondary compression increases to $4.3\times\dot{v}_0$ and $11.9\times\dot{v}_0$, respectively. As it can be observed in Fig. 5, the proposed analysis predicts also with the remarkable accuracy on the volumetric strain-time curves due to different soil parameters. This may be due to fit the calculated volumetric strain-time curves to the observed ones at

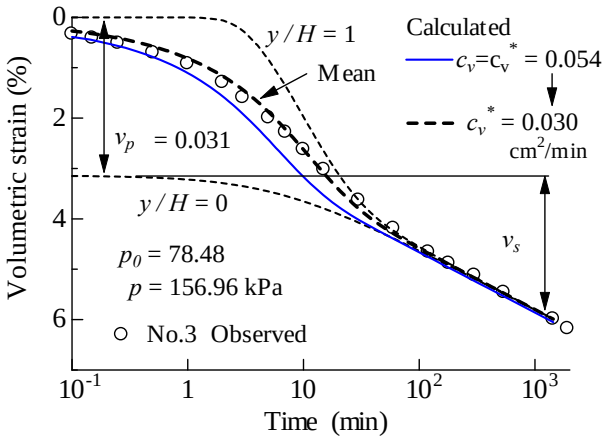

Fig. 3 Consolidation-time curves with different c_v^*

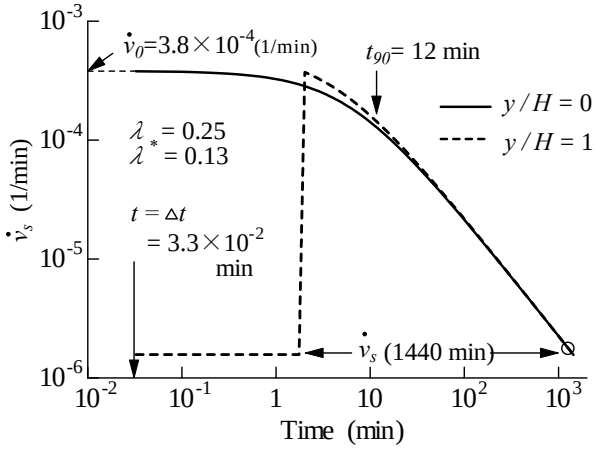

Fig. 4 Relation between the rate of secondary compression $\dot{v}_s$ and time calculated for sample No. 3

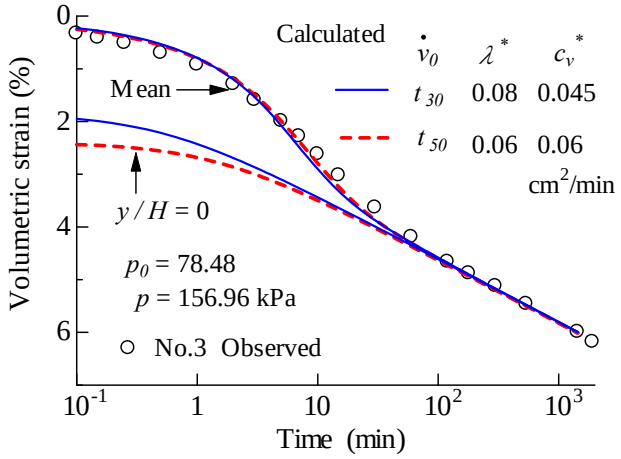

Fig. 5 Consolidation-time curves with different $\dot{v}_0$

the elapsed time t_f = 1440 min. It is apparent from Fig. 5 that the increase in $\dot{v}_0$ needs to change the values of the other parameters, λ^* and c_v^* indicated in this figure and this leads to the reduction of primary compression. However, it should be noted that adoptions of the appropriate value of soil parameters are not based on the experimental evidence because it is impossible to measure the secondary compression during primary consolidation. The ratios of primary to total compressibility λ^* / λ (= 0.2 to 0.5) express the importance of the assumption for $\dot{v}_0$.

Secondary compression constitutes approximately 50% to 80% (λ^* / λ = 0.2 to 0.5) of total compression. It is also clear that the assumption of the initial rate of secondary compression value affects predominately on both the rate and magnitude of one-dimensional consolidation. The time increment Δt used in finite difference consolidation analysis is limited (or restricted) by the spatial grid increment Δy.

(3) The maximum drainage distance H

The assumption of the value of $\dot{v}_0$ is also dependent on the sample thickness. The time increment in the analysis of thick field deposits may be considerably greater than that of the thin laboratory sample. It is important to consider how to postulate the value of $\dot{v}_0$ at the time increment Δt. The relationship between the initial rate of secondary compression and the maximum drainage distance H is given by

$$\dot{v}_{0F} = \frac{\dot{v}_{0L}}{\left(\frac{H_F}{H_L}\right)^n} \tag{10}$$

where n is the index of a fixed number, suffix L and F refer to thin laboratory sample and thick field deposit respectively.

The results of numerical analysis for the special case in which n = 0 or n = 2 and H = 0.88 or 8.8 cm are shown in Fig. 6. The basic soil parameters (No. 3 in Table 1 and Fig. 3) were used to calculate the consolidation-time curves of a thick sample based on the same conditions as a thin sample. Dash lines with n = 0 for thin and thick samples merge onto the same secondary compression-time curve. However, the solid line calculated with n = 2 can be simply displaced in proportional to a H^2 scaling method.

Figure 7 shows the relationships of the volumetric strain-time curve which refer to the consolidation of clay samples with different thickness. The experimental result with the drainage distance shorter than 1 cm seems to be closer to hypothesis A. Assuming n = 2 in Eq. (10), there are reasonable agreements between observed and calculated volumetric strain-time curves. Observed curves support hypothesis A and do not coincide with one line in the range of secondary compression as shown in Suklje's isotaches theory (Suklje 1969).

Table 2 shows soil parameters obtained from the consolidation-time curve in Fig. 1 and also Fig. 8 which represents the observation in one-dimensional consolidation test of clay layers with different thickness conducted by Aboshi (1973). The consolidation-time curves of the large specimens H_L = 10 cm are calculated by using the value of n = 2 (solid line) and n = 0 (dash line) in Eq. (10). As compared with the observations, the numerical results with n = 2 appears to give reliable prediction. As results, it can be concluded that the consolidation-time curve with the different thickness of the clay layer is sensitively influenced by the assumption of the initial rate of secondary compression.

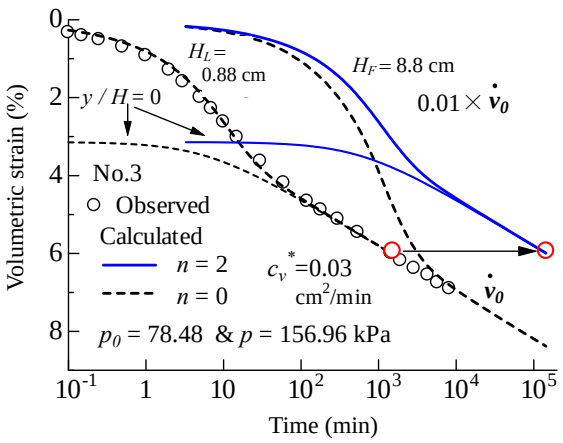

Fig. 6 Consolidation-time curves with different *H*

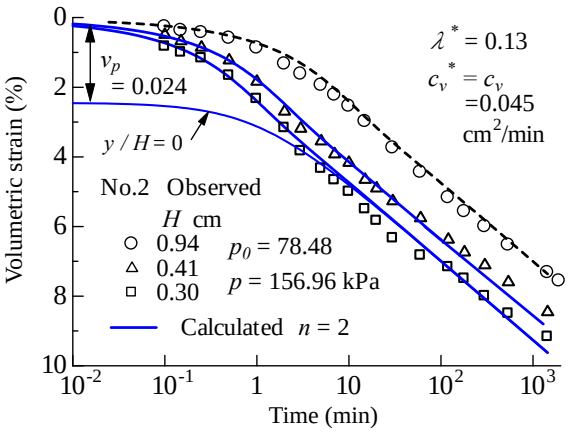

Fig. 7 Comparison of observed and calculated results with different *H*

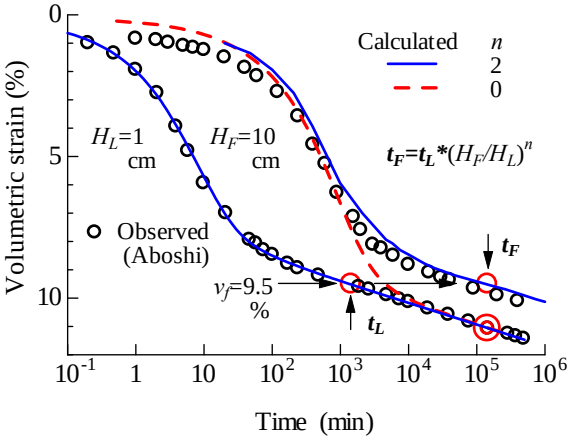

Fig. 8 Calculation results changed coefficient *n* using the one-dimensional consolidation results with different thickness conducted by Aboshi (1973)

Table 2 Soil parameters (after Aboshi 1973)

λ	λ^*	c_v (cm²/min)	α (%)	$\dot{v}_0$ (1/min)	t_{90} (min)	p_0 (kPa)	p (kPa)
0.41	0.25	0.06	0.77	2.3×10^{-4}	14.4	19.62	39.24

4. CONCLUSIONS

One-dimensional consolidation analysis taking into account of secondary compression has been developed for normally consolidated clay. A fitting procedure is suggested for obtaining the soil parameters for the analysis from the experimental results. The following conclusions can be drawn from the comparison of the calculated and observed secondary compression behaviors.

1. When large amount of secondary compression occurs during the primary consolidation, it is impossible to determine some of the soil parameters defined by the primary compression.
2. The assumption for the initial rate of secondary compression $\dot{v}_0$ has a predominant influence on the calculated consolidation-time curve.
3. Predictions using such soil parameters without experimental evidence agree well with the observed consolidation-time curve.
4. The calculated consolidation-time curves are influenced by the assumption of the initial rate of secondary compression and do not coincide in one line on the secondary consolidation stage as shown in Suklje's isotaches theory.

NOTATIONS

The following symbols are used in this paper.

c_v^*	coefficient of consolidation defined by the primary consolidation (cm^2/min)
$\dot{e}$	void ratio rate
f_0	initial specific volume
H_F	maximum drainage distance of thick field sample (cm)
H_L	maximum drainage distance of thin laboratory sample (cm)
k	permeability of soil (cm/min)
p	vertical effective stress (kPa)
p_0	vertical effective overburden stress (kPa)
t_{EOP}	end of primary consolidation (min)
u	excess pore water pressure (kPa)
$\dot{v}$	time rate of the total volumetric strain (1/min)
$\dot{v}_p$	time rate of the primary volumetric strain (1/min)
$\dot{v}_s$	time rate of the secondary volumetric strain (1/min)
$\dot{v}_0$	initial rate of the secondary volumetric strain (1/min)
w_L	liquid limit (%)
w_n	natural water content (%)
w_p	plastic limit (%)
y	vertical coordinate (cm)
α	coefficient of secondary compression defined by the volumetric strain (%)
γ_w	unit weight of water (gf/cm^3)
λ	compression index
λ^*	compression index defined by the primary compression
ρ	soil particle density (g/cm^3)

REFERENCES

Aboshi, H. (1973). "An experimental investigation on similitude in the consolidation of a soft clay, including the secondary creep settlement." *Pro. 8th Int. Conf. on SMFE*, Specialty Session 2, **4**(3), 88.

Feng, T. W. (2010). "Some observations on the oedometric consolidation strain rate behaviors of saturated clay." *Journal of GeoEngineering*, TGS, **5**(1), 1–7.

Haan, E. D. and Kamao, S. (2003). "Obtaining isotache parameters from a C.R.S. K_0-oedometer." *Soils and Foundations*, **43**(4), 203–214.

Harr, M. D. (1966). *Foundation of Theoretical Soil Mechanics*, McGraw hill Book Company, 136.

Inada, M. and Akaishi, M. (1980). "One-dimensional consolidation analysis taking account of dilatancy." *Soils and Foundations*, **20**(2), 119–127 (in Japanese).

Ladd, C. C., Foott, R., Ishihara, K., Schlosser, F., and Poulos, H. G. (1977). "Stress-deformation and strength characteristics." *State of the Art Report*, *Proc. 9th Int. Conf. on SMFE*, Tokyo, **2**, 421–494.

Leroueil, S., Kabbaj, M., Tavenas, F., and Bouchard, R. (1985). "Stress-strain-strain rate relation for the compressibility of sensitive clays." *Geotechnique*, **35**(2), 159–180.

Mesri, G. and Rokhsar, A. (1974). "Theory of consolidation for clays." *ASCE, Journal of the Geotechnical Engineering Division*, **100**, GT8, 889–904.

Mesri, G., Feng, T. W., and Shahien, M. (1995). "Compressibility parameters during primary consolidation." *Invited Lecture, Proc. of the Int, Symp, on Consolidation of Clayey Soils*, IS-Hiroshima, **2**, 1021–1038.

Murakami, Y. (1977). "Effects of loading duration on results of one-dimensional consolidation test." *Soils and Foundations*, **17**(4), 59–69.

Nash, D. (2001). "Modelling the effects of surcharge to reduce long term settlement of reclamations over soft clays. — A numerical case study." *Soils and Foundations*, **41**(5), 1–13.

Sekiguchi, H. and Torihara, M. (1976). "Theory of one-dimensional consolidation of clays with consideration of their rheological properties." *Soils and Foundations*, **16**(1), 27–44 (in Japanese).

Shirako, H., Sugiyama, M., Akaishi, M., and Tonosaki, A. (2008). "Estimation of secondary compression during primary consolidation." *Journal of Japan Society of Civil Engineers*, Ser. C, **64**(3), 556–570 (in Japanese).

Suklje, L. (1969). *Rheological Aspect of Soil Mechanics*. John Wiley and Sons, New York.

Takeda, T., Sugiyama, M., Akaishi, M., and Chang, H. W. (2012). "Secondary compression behavior in one-dimensional consolidation test." *Journal of GeoEngineering*, TGS, **7**(2), 53–58.

Tatta, N., Inagaki, M., Mishima, N., Fujiyama, T., Ishiguro, T., and Ohta, T. (2003). "Prediction of long term deformation of road embankment on soft ground by FEM and its application to performance design." *Journal of Japan Society of Civil Engineers*, **743**(3), 173–187 (in Japanese).

Taylor, D. W. (1948). *Fundamentals of Soil Mechanics*, John Wiley and Sons, New York.

Terzaghi, K. (1943). *Theoretical Soil Mechanics*, John Wiley and Sons, New York.

Yin, J. H. and Graham, J. (1996). "Elasto visco-plastic modelling of one-dimensional consolidation." *Geotechnique*, **46**(3), 515–527.